Supporting Information

Hierarchical-Metal-Organic frameworks templated $Cu_{0.5}Zn_{0.5}In_2S_4$-rGO-g-C_3N_4: flexible synthesis and enhanced photocatalytic activity

Mei-Ling Xu[a,b], Ling-Wang Liu[a], Kai Wang[a], Yi-Chuan Dou[a], Kui Li[a,*], Xin Cheng [b,*] and Feng-Ming Zhang[c,*]

[a]School of Materials Science and Engineering, University of Jinan, Jinan 250022, China

[b]Shandong Provincial Key Laboratory of Preparation and Measurement of Building Materials, University of Jinan, Jinan, 250022, China

[c]School of Materials Science and Engineering, College of Chemical and Environmental Engineering, Harbin University of Science and Technology, Harbin 150040, China

Email: mse_lik@ujn.edu.cn, ujn_chengxin@163.com, zhangfm80@163.com.

Experimental Procedures

Synthesis of CuZnIn-HMOFs with different ratio of the MIM and PTA

In the typical fabrication procedure of HMOFs, suitable amounts of $Zn(NO_3)_2 \cdot 6H_2O$, $Cu(NO_3)_2 \cdot 3H_2O$, $In(NO_3)_3$, 2-Methylimidazole (MIM) and P-Phthalic acid (PTA) were dissolved in 20 mL of N, N-Dimethylformamide (DMF), followed by ultrasonication for 30 min. Then, the obtained mixed solution was transferred to a 50 mL Teflon-lined stainless-steel autoclave, which was heated to 100 °C for 24 h. After cooling to room temperature, the as-synthesized precipitates were rinsed three times with DMF and dried at 60 °C overnight in air. The theoretical molar ratios of MIM/PTA were 1:0, 99.7:0.3, 99.5:0.5, 99.1:0.9, 98.8:1.2, 97:3, 95:5, 9:1, 7:3, 5:5, 3:7 and 0:1.

Synthesis of Cu-Zn-In-S and its heterostructures

Typically, 100 mg of the as-prepared CuZnIn-HMOFs with different ratio of the MIM and PTA and thioacetamide (TAA) (120 mg) were dissolved into 20 mL DMF solvent and treated at 40 ºC for 24 h under stirring. Then, the obtained precursors rinsed three times with DMF, and then were dispersed into 30 mL DMF, after the continuous stirring for 30 min, the above suspension into 50 mL Teflon-lined stainless steel autoclave, followed by heating at 140 °C for 12 h. The hollow sulfide was centrifuged, washed three times with ethanol and deionized water, and dried at 60 ºC overnight.

Synthesis of the physical mixture of $Cu_{0.5}Zn_{0.5}In_2S_4$+rGO+g-C_3N_4

Briefly, the GO (0.5 mg) was dispersed in deionized water (30 mL) in an ice water bath (0 °C) by ultrasonication for 10 min to form a homogeneous solution. Then an aqueous solution of $NaBH_4$ (1 mL, 20 mM) was added dropwise to the above solution under vigorous stirring, and then the solutions were stirred for another 1 h at 0 °C. The final product of rGO was collected by centrifugation. Then, the optimal ratio of $Cu_{0.5}Zn_{0.5}In_2S_4$ (100 mg), g-C_3N_4 (30 mg) and rGO were physically mixed, and the physical mixture was marked as $Cu_{0.5}Zn_{0.5}In_2S_4$+rGO+g-C_3N_4.

Characterization

The powder X-ray diffraction (XRD) patterns were recorded on a D/max 2500 VL/PC diffractometer (Japan) equipped with graphite monochromatized Cu Kα radiation (λ = 1.54060 Å), and the corresponding work voltage and current was 40 kV and 100 mA, respectively. Fourier transform infrared spectroscopy (FTIR) was collected on a Thermo Scientific Nicolet iS10 spectrometer. The transmission electron microscopy (TEM), elemental mapping and high-resolution TEM (HRTEM) images were recorded on JEOL-2100F apparatus at an accelerating voltage of 200 kV. Scanning electron microscope (SEM, JSM-7600F) were performed at an acceleration voltage of 10 kV, and the elemental mapping was performed with JSM-5160LV-Vantage typed energy dispersive X-ray spectroscopy (EDS) spectrometer. Raman spectroscopy was recorded on a LabRAM HR Evolution with 325 nm laser. Thermal stability was checked by thermogravimetric analysis (TGA) using NETZSCH STA 449F thermal analyzer in the temperature range of 30-1000 °C at a heating rate of 10 °C min^{-1} under Ar flow. The X-ray photoelectron spectroscopy (XPS) was conducted on an ESCALAB 250 Xi (USA)-ray photoelectron spectrometer using Al as the excitation source. Element content analysis was tested on an inductively coupled plasma (ICP) spectroscope (Agilent ICP0ES730, America). Electron Paramagnetic Resonance (EPR) responses of $Cu_{0.5}Zn_{0.5}In_2S_4$-rGO-g-C_3N_4 was conducted in pure water using 5,5-Dimethyl-1-pyrroline N-oxide (DMPO) as the spin trapping agent. The UV−Vis absorption and diffused reflectance spectra were recorded using a Cary 5000 UV-Vis spectrometer (Viarian, USA) with $BaSO_4$ as a reflectance standard. Nitrogen adsorption-desorption isotherms were measured on a Quantachrome Instruments Autosorb AS-6B. Steady photoluminescence (PL) emission spectra were tested by a luminescmce spectrophotometer (QM-400, PTI) with 350 nm excitation wavelength. The fluorescence decay times were measured using the Horiba Jobin Yvon Data Station HUB operating in time-correlated single photon counting mode (TCSPC) with the time resolution of 200 ps. Nano LED diode emitting pulses at 370 nm with 1 MHz repetition rate was used as an excitation source. Light-scattering Ludox solution was used to obtain the instrument response function (prompt). The time ranges are 0.055 ns/channel in 4096 effective channels. All the electrochemical experiments were conducted on the electrochemical station (Bio-Logic SP-150) in a three-electrode system at room temperature with a glassy carbon electrode (3 mm in

diameter), (sheet resistance 20−25 Ω/square) as the working electrode, a carbon rod as the counter electrode, and an Ag/AgCl electrode as the reference electrode.

Photocatalytic Hydrogen Production

The photocatalytic H_2-production experiments were performed via a photocatalytic H_2-production activity evaluation system (CEL-SPH2N, CEAULight, China) in a 300 mL Pyrex flask, and the openings of the flask were sealed with silicone rubber septum. A 300 W xenon arc lamp through a UV-cutoff filter with a wavelength range of 420 ~ 800 nm with focused intensity on the flask of ~ 200 $mW \cdot cm^{-2}$, was used as a visible light source to trigger the photocatalytic reaction. In a typical photocatalytic H_2-production experiment, 20 mg of the as-prepared photocatalyst was suspended in 50 mL of mixed aqueous solution (0.35 M Na_2S and 0.25 M Na_2SO_3). Before irradiation, the system was vacuumed for 5 min via the vacuum pump to completely remove the dissolved oxygen and ensure the reactor was in an anaerobic condition. A continuous magnetic stirrer (800 r/min) was applied at the bottom of the reactor to keep the photocatalyst particles in suspension during the experiments. H_2 content was analyzed by gas chromatography (GC-7900, CEAULight, China). The photocatalytic hydrogen production in pure water was performed in pure water under visible light irradiation, and the concentration of H_2O_2 was determined by a colorimetric titration method based on the formation of a yellow coloured complex Ti^{IV}–H_2O_2, using a UV/Vis spectrophotometer at 410 nm as reported in previous publication.[1] The apparent quantum efficiencies (AQEs) are presented in Table S1.

Supporting Figures

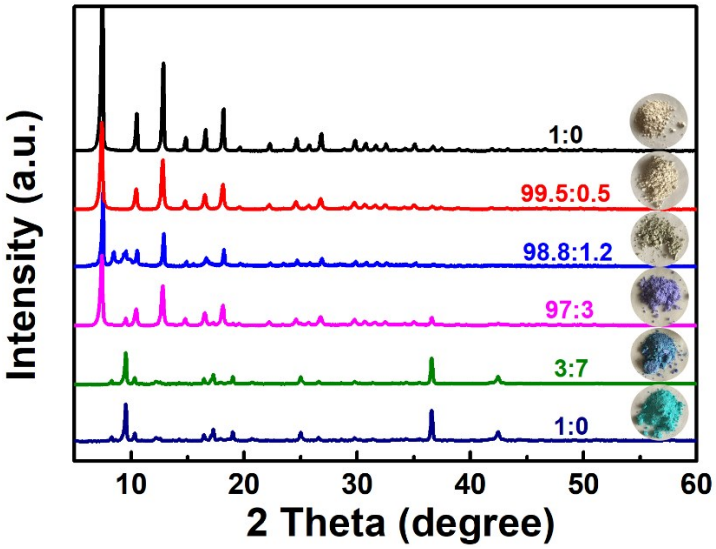

Fig. S1 XRD spectra and the color (inset) of the CuZnIn-MOFs prepared with different molar ratio of MIM/PTA.

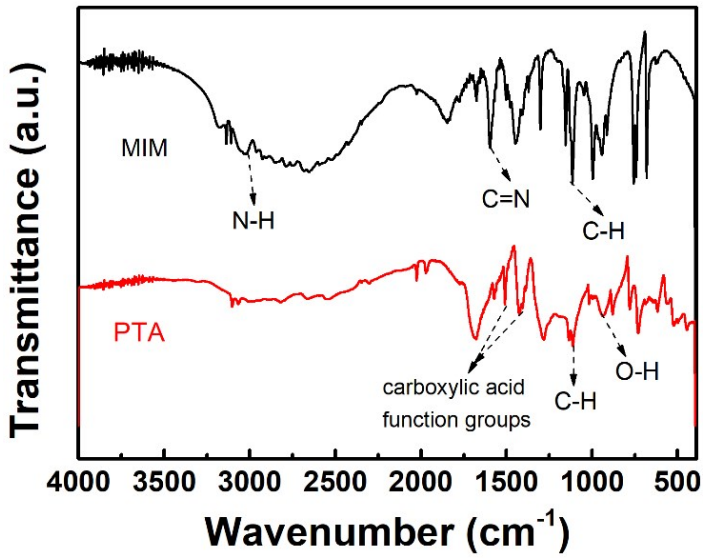

Fig. S2 FTIR spectra of pure MIM and PTA.

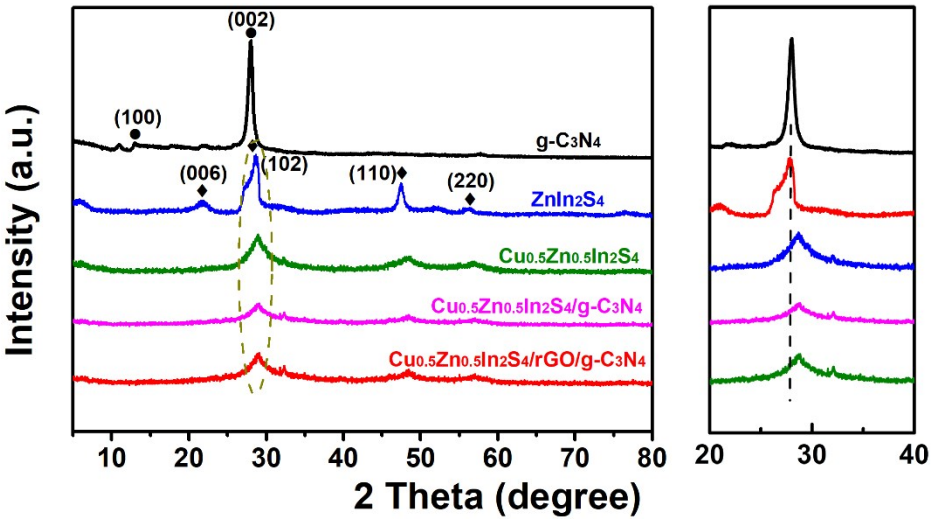

Fig. S3 The XRD patterns of the g-C_3N_4, sulfides, and $Cu_{0.5}Zn_{0.5}In_2S_4$-based heterostructure derived from the HMOF using dual ligands.

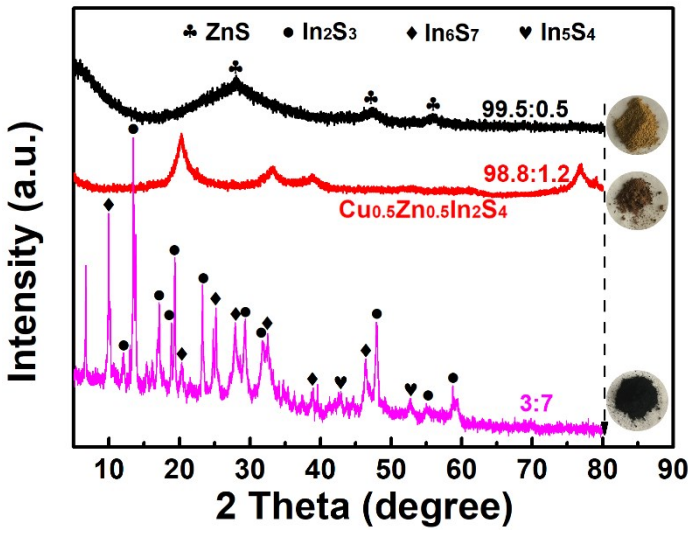

Fig. S4 XRD spectra and the color (inset) of the Cu-Zn-In-S sulfides derived from different CuZnIn-MOFs.

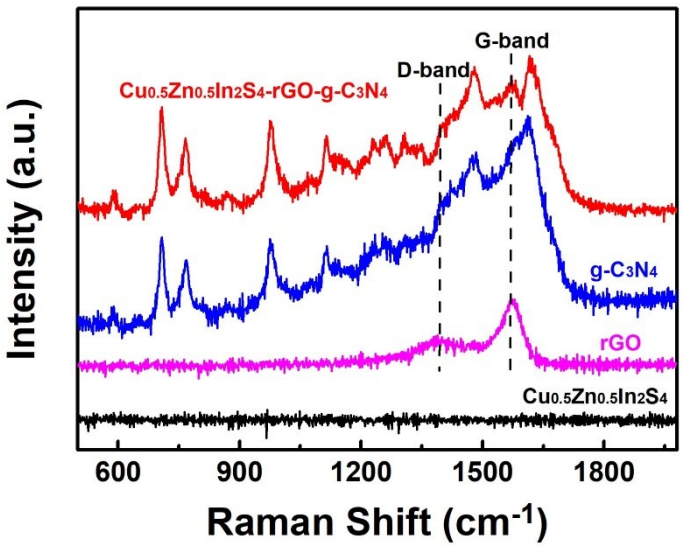

Fig. S5 Raman spectra of $Cu_{0.5}Zn_{0.5}In_2S_4$, g-C_3N_4, rGO and $Cu_{0.5}Zn_{0.5}In_2S_4$-rGO-g-C_3N_4.

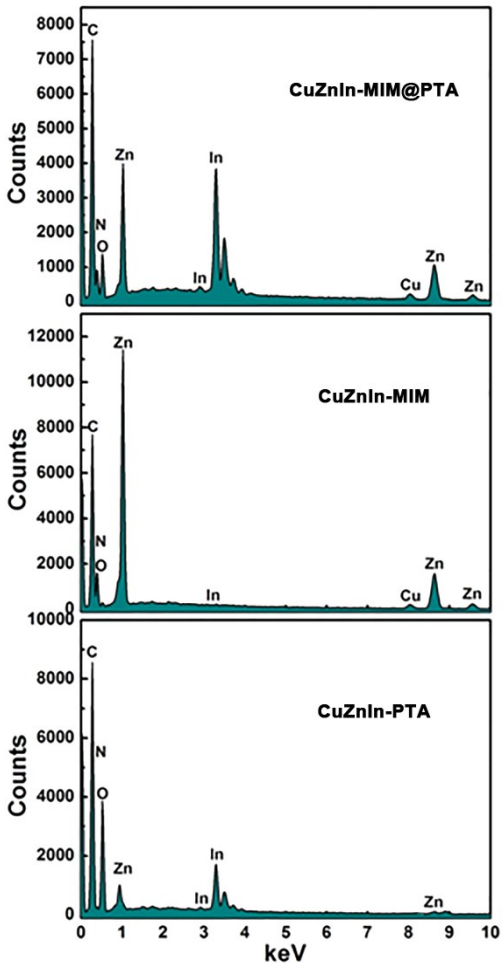

Fig. S6 EDS spectra of (a) CuZnIn-MIM, (b) CuZnIn-PTA and (c) CuZnIn-MIM@PTA.

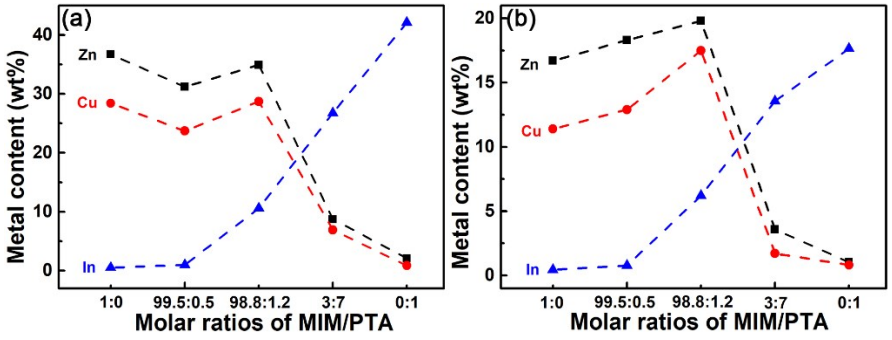

Fig. S7 Metal contents in the (a) CuZnIn-MOFs with different molar ratio of MIM/PTA and (b) Cu-Zn-In-S sulfides derived from CuZnIn-MOFs.

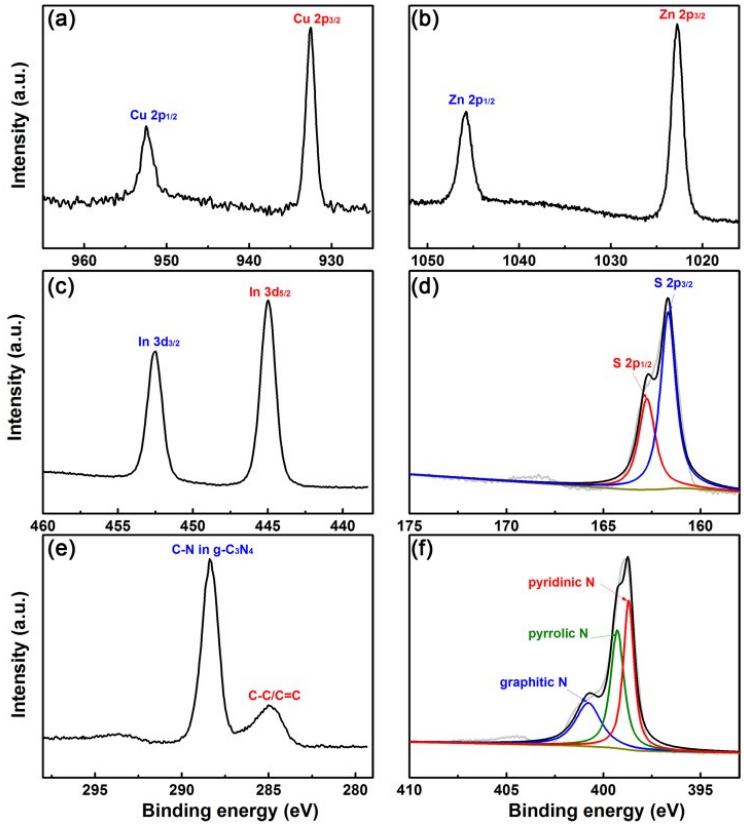

Fig. S8 High-resolution XPS spectra of (a) Zn 2p, (b) Cu 2p, (c) In 3d, (d) S 2p, (e) C 1s, (f) N 1s.

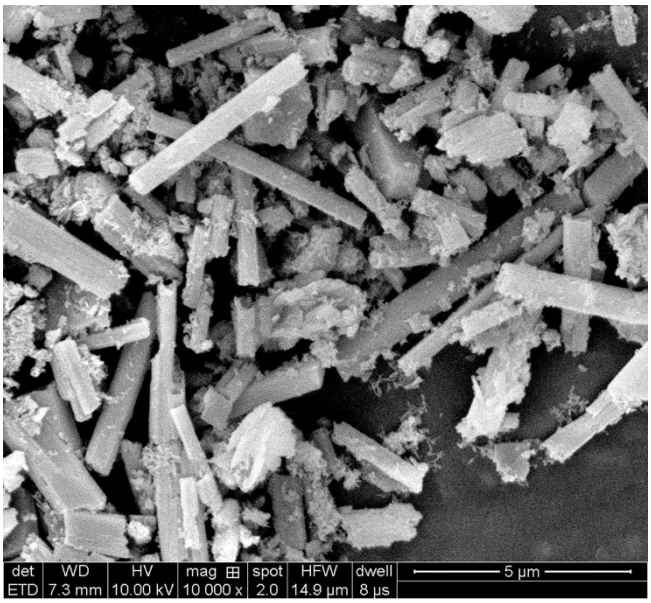

Fig. S9 SEM image of CuZnIn-PTA derived from PTA ligand.

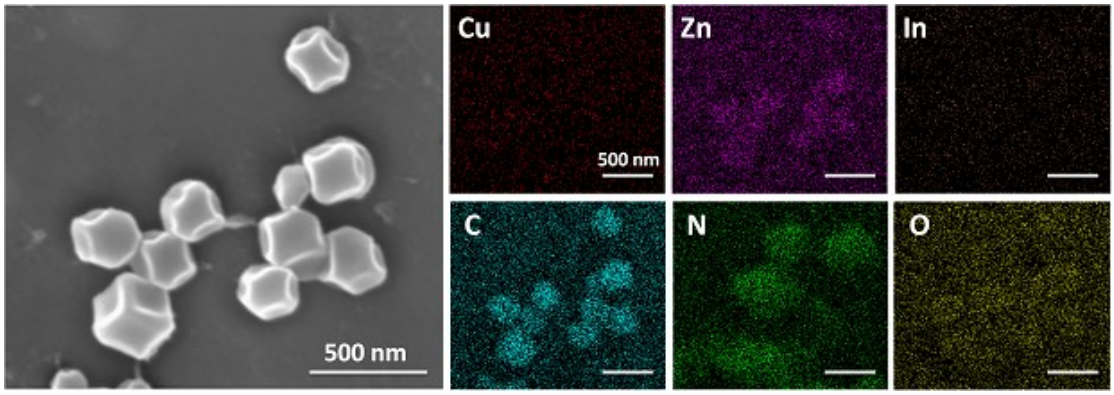

Fig. S10 Elemental mapping images of CuZnIn-MIM derived from MIM ligand. The In concentration of the In was very low owing to the poor coordination between In and MIM.

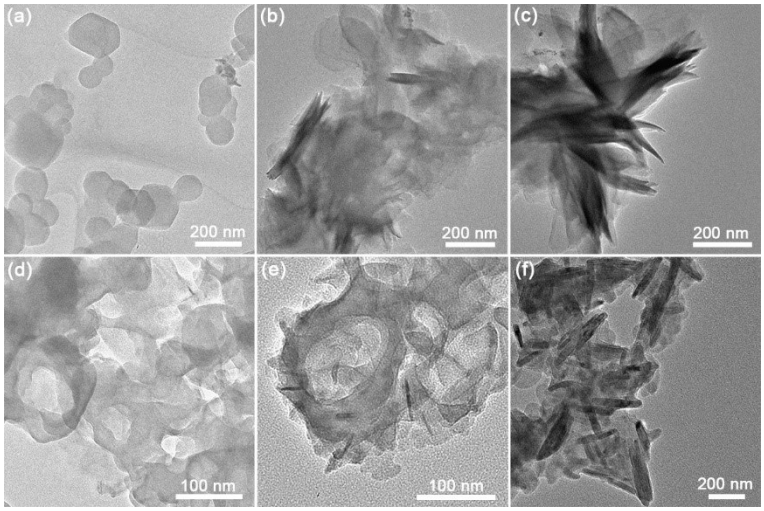

Fig. S11 TEM images of the CuZnIn-MOFs with different MIM/PTA molar ratio of (a) 98.8:1.2, (b) 97:3 and (c) 3:7 and corresponding sulfides of (d) 98.8:1.2, (e) 97:3 and (f) 3:7.

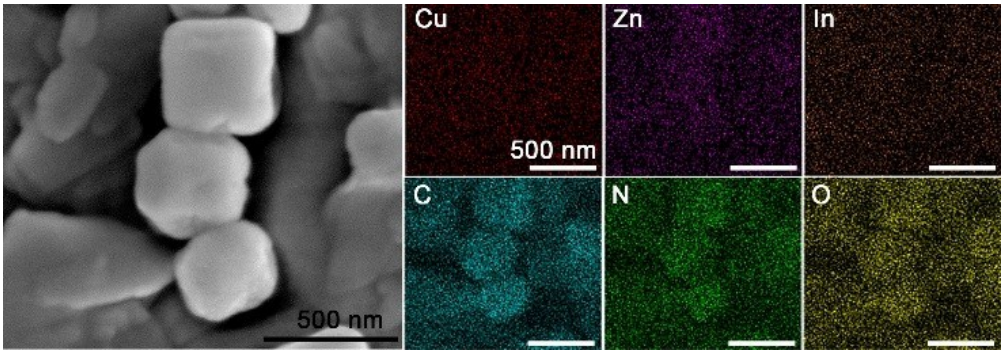

Fig. S12 The SEM image and the elemental mapping of the CuZnIn-HMOFs (CuZnIn-MIM@PTA). All the elements of Cu, Zn, In, C, N and O distributed uniformly all through the skeleton of the HMOFs.

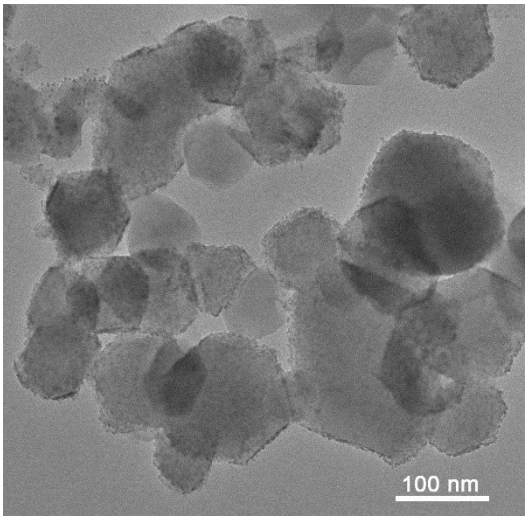

Fig. S13 TEM image of $Cu_{0.5}Zn_{0.5}In_2S_4$.

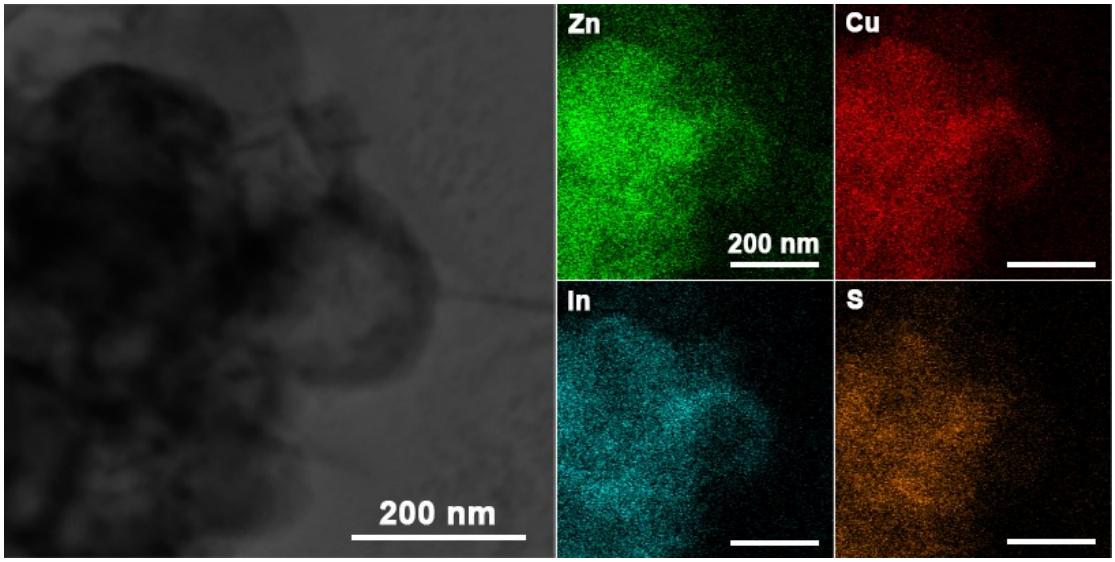

Fig. S14 The TEM image and the elemental mapping of the $Cu_{0.5}Zn_{0.5}In_2S_4$ derived from CuZnIn-HMOFs.

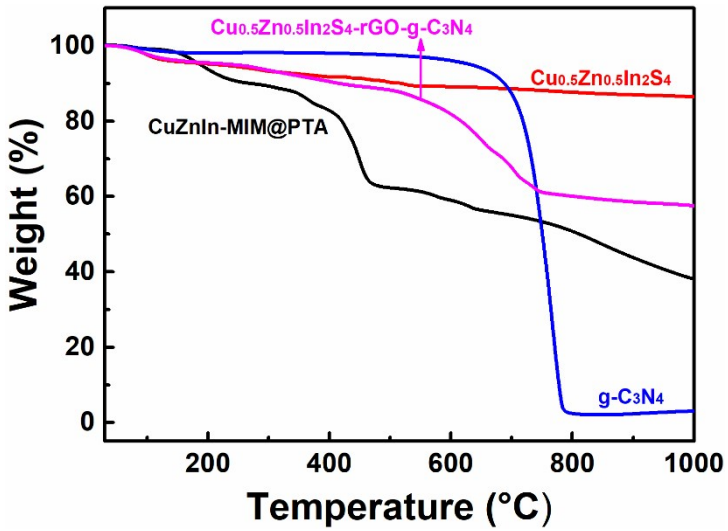

Fig. S15 TGA curves of CuZnIn-MIM@PTA, $Cu_{0.5}Zn_{0.5}In_2S_4$, g-C_3N_4 and $Cu_{0.5}Zn_{0.5}In_2S_4$-rGO-g-C_3N_4.

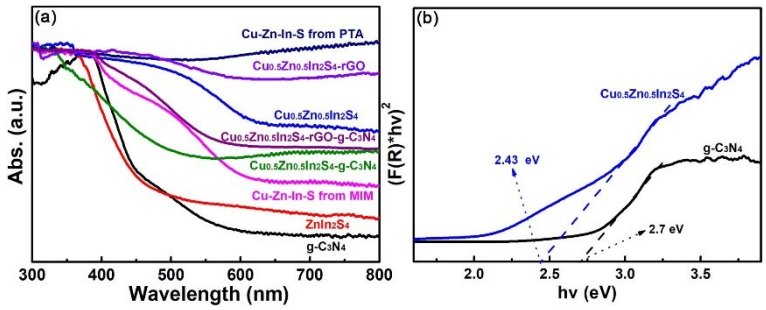

Fig. S16 (a) UV-vis diffuse absorption spectra of g-C_3N_4, $ZnIn_2S_4$, $Cu_{0.5}Zn_{0.5}In_2S_4$, Cu-Zn-In-S MIM, Cu-Zn-In-S PTA, $Cu_{0.5}Zn_{0.5}In_2S_4$-g-C_3N_4, $Cu_{0.5}Zn_{0.5}In_2S_4$-rGO and $Cu_{0.5}Zn_{0.5}In_2S_4$-rGO-g-C_3N_4 samples and estimated band gaps (b) of g-C_3N_4 and $Cu_{0.5}Zn_{0.5}In_2S_4$ samples.

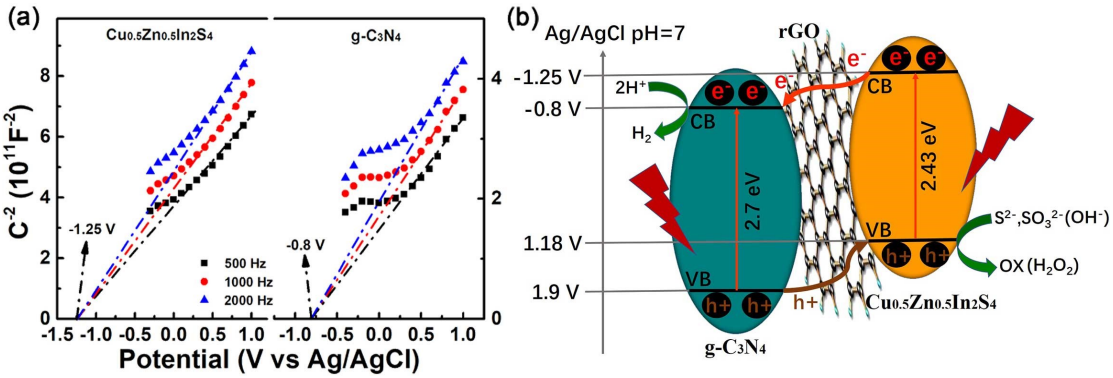

Fig. S17 Mott−Schottky plots of the (a) g-C_3N_4 and $Cu_{0.5}Zn_{0.5}In_2S_4$ derived from the HMOFs, and the (b) band structure matching between g-C_3N_4, rGO and $Cu_{0.5}Zn_{0.5}In_2S_4$.

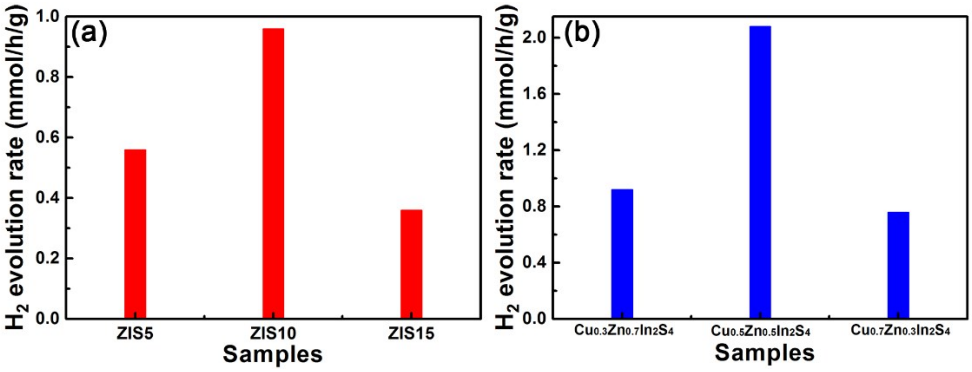

Fig. S18 Comparison of the photocatalytic H_2-production rates of (a) $ZnIn_2S_4$ with different the amounts of In and (b) $Cu_{0.5}Zn_{0.5}In_2S_4$ with different Cu/Zn ratios from 0.35 M Na_2S and 0.25 M Na_2SO_3 mixed aqueous solutions under visible light (λ > 420 nm).

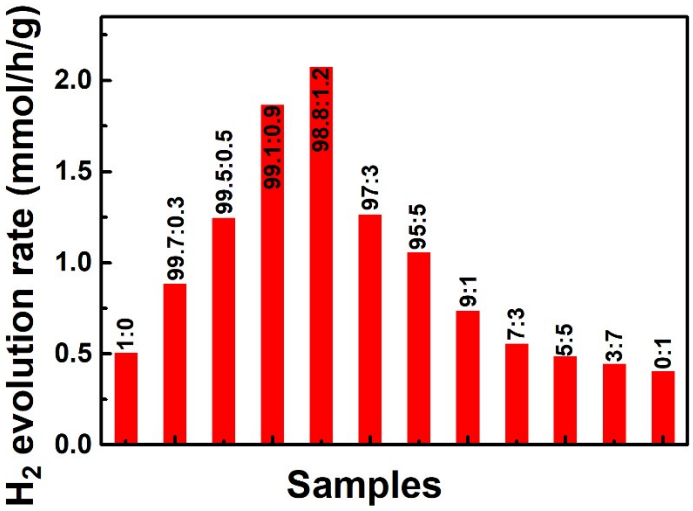

Fig. S19 Comparison of the photocatalytic H_2-production rates of the Cu-Zn-In-S sulfides derived from different CuZnIn-MOFs.

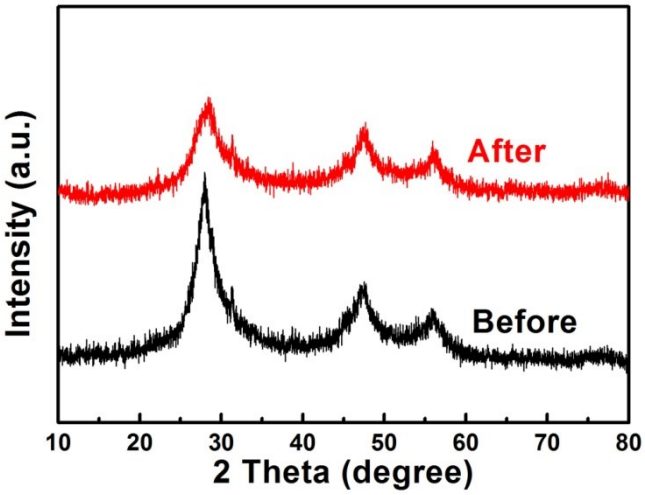

Fig. S20 XRD patterns of $Cu_{0.5}Zn_{0.5}In_2S_4$ before and after photocatalytic reaction of 30 h.

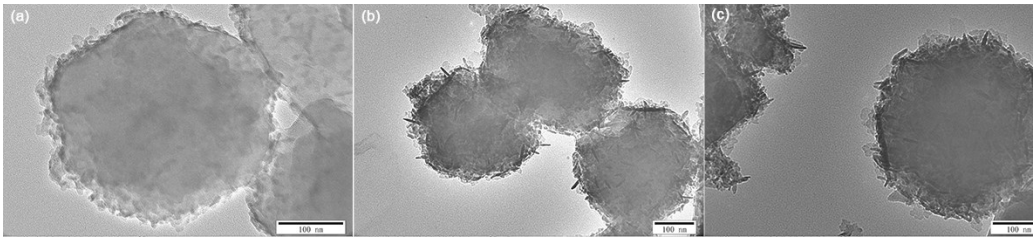

Fig. S21 TEM images of (a) $Cu_{0.5}Zn_{0.5}In_2S_4$, (b) $Cu_{0.5}Zn_{0.5}In_2S_4$-g-C_3N_4 and (c) $Cu_{0.5}Zn_{0.5}In_2S_4$-rGO-g-C_3N_4 after the HER reaction.

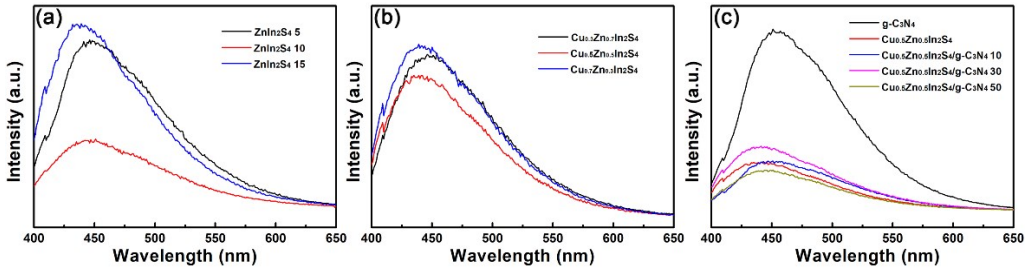

Fig. S22 PL spectra of (a) $ZnIn_2S_4$ with different the amounts of In, (b) $Cu_{0.5}Zn_{0.5}In_2S_4$ with different the molar ratio of Cu/Zn, and (c) $Cu_{0.5}Zn_{0.5}In_2S_4$-g-C_3N_4 with different amount of g-C_3N_4.

Supporting Table

Table S1. Calculated apparent quantum efficiency (AQE) of CZIS-I, $Cu_{0.5}Zn_{0.5}In_2S_4$, $Cu_{0.5}Zn_{0.5}In_2S_4$-g-C_3N_4 and $Cu_{0.5}Zn_{0.5}In_2S_4$-rGO-g-C_3N_4 samples at different wavelengths.

Samples	Wavelength (nm)	H_2 Evolved (μmol)	Light Intensity (mW)	AQY (%)
CZIS-1	420	0.72	13.1	0.87
$Cu_{0.5}Zn_{0.5}In_2S_4$	420	7.4	13.1	8.94
$Cu_{0.5}Zn_{0.5}In_2S_4$-g-C_3N_4	420	23.67	13.1	28.61
$Cu_{0.5}Zn_{0.5}In_2S_4$-rGO-g-C_3N_4	420	43.27	13.1	52.3
	475	26.35	18.4	22.67
	550	5.51	20.3	3.28
	650	3.29	16.5	2.04

λ=420 nm

CZIS-I:

$$N = \frac{E\lambda}{hc} = \frac{13.1 \times 10^{-3} \times 3600 \times 420 \times 10^{-9}}{6.626 \times 10^{-34} \times 3 \times 10^{8}} = 9.96 \times 10^{19}$$

$$AQE = \frac{the\ number\ of\ reacted\ electrons}{the\ number\ of\ incident\ photons} \times 100\%$$

$$= \frac{2 \times the\ number\ of\ evolved\ H_2\ molecules}{N} \times 100\%$$

$$= \frac{2 \times 6.02 \times 10^{23} \times 0.72 \times 10^{-6}}{9.96 \times 10^{19}} = 0.87\%$$

$Cu_{0.5}Zn_{0.5}In_2S_4$:

$$N = \frac{E\lambda}{hc} = \frac{13.1 \times 10^{-3} \times 3600 \times 420 \times 10^{-9}}{6.626 \times 10^{-34} \times 3 \times 10^{8}} = 9.96 \times 10^{19}$$

$$AQE = \frac{the\ number\ of\ reacted\ electrons}{the\ number\ of\ incident\ photons} \times 100\%$$

$$= \frac{2 \times the\ number\ of\ evolved\ H_2\ molecules}{N} \times 100\%$$

$$= \frac{2 \times 6.02 \times 10^{23} \times 7.4 \times 10^{-6}}{9.96 \times 10^{19}} = 8.94\%$$

$Cu_{0.5}Zn_{0.5}In_2S_4$-g-C_3N_4:

$$N = \frac{E\lambda}{hc} = \frac{13.1 \times 10^{-3} \times 3600 \times 420 \times 10^{-9}}{6.626 \times 10^{-34} \times 3 \times 10^8} = 9.96 \times 10^{19}$$

$$AQE = \frac{the\ number\ of\ reacted\ electrons}{the\ number\ of\ incident\ photons} \times 100\%$$

$$= \frac{2 \times the\ number\ of\ evolved\ H_2\ molecules}{N} \times 100\%$$

$$= \frac{2 \times 6.02 \times 10^{23} \times 23.67 \times 10^{-6}}{9.96 \times 10^{19}} = 28.61\%$$

$Cu_{0.5}Zn_{0.5}In_2S_4$-rGO-g-C_3N_4:

$$N = \frac{E\lambda}{hc} = \frac{13.1 \times 10^{-3} \times 3600 \times 420 \times 10^{-9}}{6.626 \times 10^{-34} \times 3 \times 10^8} = 9.96 \times 10^{19}$$

$$AQE = \frac{the\ number\ of\ reacted\ electrons}{the\ number\ of\ incident\ photons} \times 100\%$$

$$= \frac{2 \times the\ number\ of\ evolved\ H_2\ molecules}{N} \times 100\%$$

$$= \frac{2 \times 6.02 \times 10^{23} \times 43.27 \times 10^{-6}}{9.96 \times 10^{19}} = 52.3\%$$

λ=475 nm

$Cu_{0.5}Zn_{0.5}In_2S_4$-rGO-g-C_3N_4:

$$N = \frac{E\lambda}{hc} = \frac{18.4 \times 10^{-3} \times 3600 \times 475 \times 10^{-9}}{6.626 \times 10^{-34} \times 3 \times 10^8} = 1.58 \times 10^{20}$$

$$AQE = \frac{the\ number\ of\ reacted\ electrons}{the\ number\ of\ incident\ photons} \times 100\%$$

$$= \frac{2 \times the\ number\ of\ evolved\ H_2\ molecules}{N} \times 100\%$$

$$= \frac{2 \times 6.02 \times 10^{23} \times 26.35 \times 10^{-6}}{1.58 \times 10^{20}} = 20.1\%$$

λ=550 nm

$Cu_{0.5}Zn_{0.5}In_2S_4$-rGO-g-C_3N_4:

$$N = \frac{E\lambda}{hc} = \frac{20.3 \times 10^{-3} \times 3600 \times 550 \times 10^{-9}}{6.626 \times 10^{-34} \times 3 \times 10^8} = 2.02 \times 10^{20}$$

$$AQE = \frac{the\ number\ of\ reacted\ electrons}{the\ number\ of\ incident\ photons} \times 100\%$$

$$= \frac{2 \times the\ number\ of\ evolved\ H_2\ molecules}{N} \times 100\%$$

$$= \frac{2 \times 6.02 \times 10^{23} \times 5.51 \times 10^{-6}}{2.02 \times 10^{20}} = 3.28\%$$

λ=650 nm

$Cu_{0.5}Zn_{0.5}In_2S_4$-rGO-g-C_3N_4:

$$N = \frac{E\lambda}{hc} = \frac{16.5 \times 10^{-3} \times 3600 \times 650 \times 10^{-9}}{6.626 \times 10^{-34} \times 3 \times 10^8} = 1.94 \times 10^{20}$$

$$AQE = \frac{the\ number\ of\ reacted\ electrons}{the\ number\ of\ incident\ photons} \times 100\%$$

$$= \frac{2 \times the\ number\ of\ evolved\ H_2\ molecules}{N} \times 100\%$$

$$= \frac{2 \times 6.02 \times 10^{23} \times 3.29 \times 10^{-6}}{1.94 \times 10^{20}} = 2.04\%$$

Table S2. Comparison of apparent quantum efficiencies of sulfide-based composites.

Photocatalyst	Reaction Conditions	AQE (%)	Ref.
Pt–PdS/CdS	0.5 M Na_2S and 0.5 M Na_2SO_3 aqueous	93 at 420 nm	2

	solution		
PdS/CdS	0.5 M Na_2S and 0.5 M Na_2SO_3 aqueous solution	64 at 400 nm	2
Pt–Pd/CdS	0.5 M Na_2S and 0.5 M Na_2SO_3 aqueous solution	53 at 420 nm	2
CdS–MoS_2–graphene	lactic acid (10%)	54.4 at 420 nm	3
Nanoporous CdS	0.25 M Na_2S and 0.35 M Na_2SO_3 aqueous solution	60.34 at 420 nm	4
Mo_2C/CdS	lactic acid (20%)	86 at 460 nm	5
Co(II)/CdS	0.25 M Na_2S and 0.35 M Na_2SO_3 aqueous solution	56.2 at 420 nm	6
Ni(II)/CdS	0.25 M Na_2S and 0.35 M Na_2SO_3 aqueous solution	67.5 at 420 nm	6

Table S3. Comparison of the photocatalytic H_2 generation activities of g-C_3N_4 (CN) and sulfide-based composites.

Photocatalyst	Wavelength (nm)	H_2-evolved ($mmol \cdot h^{-1} \cdot g^{-1}$)	H_2-evolved in water	Year[Ref.]
$Ni_2P/ZnIn_2S_4$	>400	2.066	/	2018[7]
MoS_2/Cu-$ZnIn_2S_4$	>420	5.463	/	2018[8]
$ZnIn_2S_4/MoSe_2$	>420	2.228	/	2017[9]

$CuInS_2$/ZnS	>400	1.59	/	2018[10]
$ZnIn_2S_4$/MoS_2-rGO	>420	0.425	/	2018[11]
CN@$ZnIn_2S_4$	>420	2.78	/	2017[12]
CN homojunction	>420	4.02	/	2016[13]
CoS_x/CN	>400	0.629	/	2017[14]
Pt@Au NRs/CN	>400	10.35	/	2019[15]
CD/CdS@MIL-101	>420	0.49	/	2019[16]
CdS NRPJs	>420	11.04	/	2016[17]
Hollow ZnCdS	>420	5.68	/	2017[18]
Hollow $Cu_{0.5}Zn_{0.5}In_2S_4$	>420	2.08	Yes	This work
$Cu_{0.5}Zn_{0.5}In_2S_4$-g-CN	>420	6.76	Yes	This work
$Cu_{0.5}Zn_{0.5}In_2S_4$-rGO-g-CN	>420	11.60	Yes	This work

Table S4. The detailed transient fluorescence properties of CZIS-I, $Cu_{0.5}Zn_{0.5}In_2S_4$, $Cu_{0.5}Zn_{0.5}In_2S_4$-g-C_3N_4, $Cu_{0.5}Zn_{0.5}In_2S_4$-rGO and $Cu_{0.5}Zn_{0.5}In_2S_4$-rGO-g-C_3N_4 samples.

Samples	A_1 (%)	τ_1 (ns)	A_2 (%)	τ_2 (ns)	A_3 (%)	τ_3 (ns)	Average lifetime τ (ns)
CZIS-I	8.24	2.37	34.42	0.78	57.34	0.34	1.12
$Cu_{0.5}Zn_{0.5}In_2S_4$	15.19	1.65	19.07	1.27	65.74	0.09	1.32
$Cu_{0.5}Zn_{0.5}In_2S_4$-g-C_3N_4	8.54	7.02	29.27	2.11	62.19	0.89	3.39
$Cu_{0.5}Zn_{0.5}In_2S_4$-rGO	0.42	0.51	0.46	1.81	0.12	7.15	4.07
$Cu_{0.5}Zn_{0.5}In_2S_4$-rGO-g-C_3N_4	10.18	3.57	84.14	0.98	5.68	11.64	5.2

Supporting References

1. X. Ye, Y. Cui, X. Qiu and X. Wang. *Appl. Catal., B.*, 2014, **152-153**, 383-389.

2. H. Yan, J. Yang, G. Ma, G. Wu, X. Zong, Z. Lei, J. Shi and C. Li. *J. Catal.*, 2009, **266**, 165-168.

3. D. Lang, T. Shen and Q. Xiang. *ChemCatChem*, 2015, **7**, 943-951.

4. N. Bao, L. Shen, T. Takata and K. Domen. *Chem. Mater.*, 2008, **20**, 110-117.

5. D. Ruan, M. Fujitsuka and T. Majima. *Appl. Catal., B.*, 2020, **264**, 118541.

6. G. Zhao, Y. Sun, W. Zhou, X. Wang, K. Chang, G. Liu, H. Liu, T. Kako and J. Ye. *Adv. Mater.*, 2017, **29**, 1703258.

7. X. L. Li, X. J. Wang, J. Y. Zhu, Y. P. Li, J. Zhao and F. T. Li. *Chem. Eng. J.*, 2018, **353**, 15-24.

8. J. R. Ran, W. W. Guo, H. L. Wang, B. C. Zhu, J. G. Yu and S. Z. Qiao. *Adv. Mater.*, 2018, **30**, 6.

9. D. Q. Zeng, L. Xiao, W. J. Ong, P. Y. Wu, H. F. Zheng, Y. Z. Chen and D. L. Peng. *Chemsuschem*, 2017, **10**, 4624-4631.

10. M. Sandroni, R. Gueret, K. D. Wegner, P. Reiss, J. Fortage, D. Aldakov and M. N. Collomb. *Energy Environ. Sci.*, 2018, **11**, 1752-1761.

11. X. Lu, J. Xie, S.-y. Liu, A. Adamski, X. Chen and X. Li. *ACS Sustain. Chem. Eng.*, 2018, **6**, 13140-13150.

12. P. Ye, X. L. Liu, J. Iocozzia, Y. P. Yuan, L. N. Gu, G. S. Xu and Z. Q. Lin. *J. Mater. Chem. A*, 2017, **5**, 8493-8498.

13. G. G. Liu, G. X. Zhao, W. Zhou, Y. Y. Liu, H. Pang, H. B. Zhang, D. Hao, X. G. Meng, P. Li, T. Kako and J. H. Ye. *Adv. Funct. Mater.*, 2016, **26**, 6822-6829.

14. J. Q. Wen, J. Xie, H. D. Zhang, A. P. Zhang, Y. J. Liu, X. B. Chen and X. Li. *ACS Appl. Mater. Interfaces*, 2017, **9**, 14031-14042.

15. L.S. Zhang, N. Ding, L.C. Lou, K. Iwasaki, H.J. Wu, Y.H. Luo, D.M. Li, K. Nakata, A. Fujishima, and Q.B. Meng, *Adv. Funct. Mater.*, 2019, **29**, 10.

16. X. B. Meng, J. L. Sheng, H. L. Tang, X. J. Sun, H. Dong and F. M. Zhang. *Appl. Catal., B.*, 2019, **244**, 340-346.

17. K. Li, M. Han, R. Chen, S. L. Li, S. L. Xie, C. Y. Mao, X. H. Bu, X. L. Cao, L. Z. Dong, P. Y. Feng and Y. Q. Lan. *Adv. Mater.*, 2016, **28**, 8906-8911.

18. J. M. Chen, J. Y. Chen and Y. W. Li. *J. Mater. Chem. A*, 2017, **5**, 24116-24125.